[CANCER RESEARCH 63, 5480–5489, September 1, 2003]

CD20-induced Lymphoma Cell Death Is Independent of Both Caspases and Its Redistribution into Triton X-100 Insoluble Membrane Rafts[1]

H. T. Claude Chan, David Hughes, Ruth R. French, Alison L. Tutt, Claire A. Walshe, Jessica L. Teeling, Martin J. Glennie, and Mark S. Cragg[2]

Tenovus Research Laboratory, Cancer Sciences Division, School of Medicine, General Hospital, Tremona Road, Southampton, SO16 6YD United Kingdom [H. T. C., D. H., R. R. F., A. L. T., C. A. W., M. J. G., M. S. C.], and Genmab, Utrecht, the Netherlands [J. L. T.]

ABSTRACT

Rituximab is routinely used for the treatment of neoplasia, although the mechanism of action remains uncertain. In the current study, CD20-induced apoptosis was investigated with a panel of anti-CD20 monoclonal antibodies (mAb) in a wide range of cell lines. A hierarchy of mAb activity was apparent, with the B1 mAb generally the most potent. Apoptosis through CD20 was dependent on the nature of mAb binding and correlated with the extent of homotypic cell adhesion induced. However, using anti-CD20 mAb, which vary in the extent to which they redistribute wild-type and mutant CD20 molecules to membrane rafts, we showed that CD20-induced apoptosis was independent of translocation to TX-100 insoluble rafts. Using crmA-transfected cells and caspase inhibitors, we showed that phosphatidylserine translocation and mitochondrial permeability transition evoked during CD20-induced apoptosis appeared caspase independent. Furthermore, in cytoplasts which lack mitochondria and in Bcl_2-transfected cells, phosphatidylserine was still translocated to the cell surface after CD20 stimulation. Together, these data imply that CD20 can evoke apoptosis without the involvement of mitochondria and caspases and irrespective of redistribution into TX-100 insoluble membrane rafts.

INTRODUCTION

The success of the chimeric anti-CD20 mAb,[3] Rituximab (Ritux), in treating B-cell disorders, such as cancer and autoimmunity, has focused attention on the precise mechanisms that make anti-CD20 mAb therapeutically effective (1–4). Several lines of evidence indicate that Ritux operates through conventional effector mechanisms measured by CDC and ADCC assays. The most conclusive support for these mechanisms comes from work in primates showing that an IgG4 variant of Ritux, unlike the chimeric IgG1 mAb, was unable to deplete normal B cells (5). In addition, FcR-bearing effectors have recently been implicated both in animal models (6) and the clinic (7). Support for the complement pathway comes from the demonstration that complement is consumed during Ritux treatment (8), that on some occasions cells remaining after treatment have increased CD59 expression (9, 10) consistent with the idea that they had been subject to complement selection and that the resistance of different lymphoma cells to Ritux *in vivo* may be related to their sensitivity to CDC *in vitro* (11). However, it is also important to note that CD20 is an antigen that can transmit intracellular signals evoking cell cycle arrest and apoptosis (12, 13), at least in some cell lines, and so this third effector mechanism cannot be ignored. Indeed, Byrd *et al.* (14) have recently shown in Ritux-treated B-CLL patients that a better clinical response and more extensive depletion of CD20-positive cells are correlated with apoptosis, as detected by caspase-3 and -9 processing.

CD20 is an unusual antigen in that it can be redistributed into TX-100 insoluble membrane rafts after cross-linking with certain mAb (15), and it has recently been suggested that membrane rafts may be important in propagating the apoptosis induced through anti-CD20 mAb (16). This notion seems reasonable because lipid rafts are generally considered to be the main signaling platforms of the cell, and their coalescence into synapses provides a rationale for how transmembrane signaling is organized within the membrane. However, it should be noted that recent work in this area has also shown that in immature B cells, the BCR is excluded from lipid rafts after ligation, and this appears to favor apoptosis as opposed to proliferation (17).

Several authors have reported that apoptosis induced by anti-CD20 mAb requires extensive cross-linking and involves the activation of caspases with the resulting cleavage of poly(ADP-ribose) polymerase (14, 18, 19). However, in some instances, these conclusions rely on experiments where high concentrations of cell-permeable caspase inhibitors, such as ZVAD-FMK, are used. It is important to note that ZVAD-FMK also inhibits noncaspase enzymes, such as cathepsins and calpains, when used at concentrations $> 10\ \mu M$, and is a poor inhibitor of some caspases, such as caspase-2 (20). Similar problems are associated with using DNA fragmentation as a measure of cell death when using caspase inhibitors, because although they may block this late stage of cell destruction, the cells may still ultimately die, *e.g.*, caspase activation and DNA fragmentation induced through BCR ligation can be inhibited by caspase inhibitors, although these cells still undergo PS flipping and the MPT, rendering them nonviable (21). In addition, these effects are often only studied in one cell line with a single anti-CD20 reagent, usually Ritux, in the presence of a hyper-cross-linking polyclonal Ab, which may reflect an unnaturally high level of cross-linking compared with that achieved *in vivo*.

Therefore, in the current study, CD20-induced apoptosis was assessed in a range of cell lines using a number of different apoptotic assays and a panel of anti-CD20 mAb in the absence of additional cross-linking. The importance of caspases in CD20-induced apoptosis was assessed using crmA-transfected cells as well as caspase inhibitors at concentrations at which they are believed to remain specific. The involvement of mitochondria in CD20-induced apoptosis was determined using mitochondria-lacking cytoplasts, Bcl_2-transfected cells, and mitochondrial assays. Furthermore, using a panel of anti-CD20 mAb, TX-100 insolubility assays, and a range of CD20 mutant molecules that do not translocate to membrane rafts after mAb ligation, we were able to address whether CD20 translocation into rafts is important for subsequent apoptosis. These experiments revealed that apoptosis induced through CD20 does not require caspase activity and that apoptosis is also independent of redistribution into TX-100 insoluble membrane rafts.

Received 4/11/03; revised 6/6/03; accepted 6/17/03.

The costs of publication of this article were defrayed in part by the payment of page charges. This article must therefore be hereby marked *advertisement* in accordance with 18 U.S.C. Section 1734 solely to indicate this fact.

[1] Supported by the Biotechnology and Biological Sciences Research Council, Cancer Research UK, and Tenovus of Cardiff.

[2] To whom requests for reprints should be addressed, at Tenovus Laboratory, Cancer Sciences Division, School of Medicine, General Hospital, Tremona Road, Southampton, SO16 6YD, United Kingdom. Fax: 44 (0) 23 80704 061; E-mail: msc@soton.ac.uk.

[3] The abbreviations used are: mAb, monoclonal antibody; Ritux, Rituximab; TX-100, Triton X-100; MFI, mean fluorescence intensity; Ab, antibody; MPT, mitochondrial permeability transition; YFP, yellow fluorescent protein; BCR, B cell receptor; PI, propidium iodide; RT-PCR, reverse transcription-PCR; MTS, 3-(4,5-dimethylthiazol-2-yl)-5-(3-carboxymethoxyphenyl)-2-(4-sulfophenyl)-2H-tetrazolium salt; NT, nontreated; FSC, forward scatter; PS, phosphotidylserine.

MATERIALS AND METHODS

Cell Lines. Cell lines were obtained from the ECACC or Genmab and were maintained in antibiotic-free RPMI 1640 with FCS (Myoclone, 10%), glutamine (2 mM), and pyruvate (1 mM; Gibco Ltd., Paisley, United Kingdom), at 37°C, 5% CO_2.

Ab Production and Labeling. The mAb used are detailed in Table 1. Hybridomas were expanded in tissue culture and purified on Protein A columns. $F(ab')_2$ fragments of IgG were produced by standard pepsin digestions (22). Fab′ was produced by reduction with 20 mM 2-mercaptoethanol for 30 min at 25°C, followed by alkylation with excess iodoacetamide. Flow cytometry and ^{125}I-labeled mAb binding were as described previously (23).

Assessment of Raft-associated Antigen by TX-100 Insolubility. As a rapid assessment of antigen presence in raft microdomains, we used a flow cytometry method based on TX-100 insolubility at low temperatures, as described previously (24). In brief, cells were washed in RPMI/1% BSA and resuspended at 2.5×10^6/ml. Cells were then incubated with FITC-conjugated mAb (10 μg/ml) for 15 min at 37°C and washed in cold PBS/1% BSA/20 mM sodium azide. One half of the sample was maintained on ice to allow calculation of 100% surface antigen levels; the other was treated with 0.5% TX-100 for 15 min on ice to determine the proportion of antigens remaining in the insoluble raft fraction. Cells were maintained at 4°C throughout the assay, washed once in PBS/BSA/azide, resuspended, and assessed by flow cytometry.

Detection of Apoptosis: Annexin V PI Assay. Cells (1×10^5) were washed and resuspended in binding buffer [10 mM HEPES (pH 7.4), 140 mM NaCl, and 2.5 mM $CaCl_2$], containing 1 μg/ml FITC-annexin V. Ten μg/ml PI were also added to the samples to distinguish between early apoptosis and secondary necrosis. Subsequently, cells were assessed by flow cytometry, as detailed by Vermes *et al.* (25).

Detection of Apoptosis: 293T Apoptosis Assay. Twenty-four h after transfection with YFP-tagged constructs, 293T cells were harvested, and expression was analyzed by flow cytometry in FL1. The cells were then added to wells of a 24-well plate (coated with 10 μg/ml Ab in PBS at 37°C for 5 h) at 2×10^5/well in 1 ml of medium. After 24 h, the cells were harvested, and the percentage of apoptotic cells was determined with PI and FSC criteria by flow cytometry.

Detection of Apoptosis: DioC6 Assay. DioC6 (Molecular Probes, Cambridge, United Kingdom) is a mitochondrial reporter dye, which determines whether cells have undergone the MPT. DioC6 (10–20 nM) was added to 2.5×10^5 cells and then incubated for 15–30 min at 37°C in the dark. The cells were pelleted, washed, and resuspended in PBS before being analyzed by flow cytometry (FL1).

Detection of Apoptosis: DNA Fragmentation Assay. Samples were assessed as detailed previously (26). Briefly, 5×10^5 cells were centrifuged for 5 min at $500 \times g$ and then washed once in PBS. The cells were then resuspended in hypotonic fluorochrome solution [50 μg/ml PI, 0.1% (w/v) sodium citrate, and 0.1% (w/v) TX-100] and incubated in the dark at 4°C overnight or 1 h at room temperature. DNA from 7500 cells was detected by flow cytometry, and the proportion of DNA giving fluorescence below the G_1-$_0$ peak was taken as a measure of apoptosis.

Clonogenic Assay. Clonogenicity of cells after treatment with various anti-CD20 mAb was assessed as follows. Cells were first diluted into 30% conditioned media at a density of 20 cells/ml. mAb (5 μg/ml) was then added to cells, and the mixture was dispensed (100 μl/well = 2 cells/well) into 48 wells of a 96-well plate (Nunc Roskilde, Denmark). Plates were then incubated at 37°C, 5% CO_2 for 8–12 days before visual inspection of colonies. Wells were scored as positive if >20 viable cells were present. The number of positive wells was then expressed as a percentage of the NT control sample according to the equation % of control = (number of colonies in treated sample/number of colonies in NT sample) × 100.

Growth Inhibition Assay. Growth inhibition was assessed using the CellTiter 96 AQueous cell proliferation assay (Promega, Madison, WI), according to the manufacturer's instructions. This method relies on the bioreduction of a modified tetrazolium compound, MTS, by viable cells to yield formazan, which can be observed by measuring absorbance at 490 nm. In brief, 100 μl of cells (2×10^5/ml) were dispensed into individual wells of a 96-well plate (Nunc) in the presence of varying concentrations of mAb. Duplicate wells of each mAb treatment were performed, and the plates were incubated at 37°C, 5% CO_2 for 48 h. Subsequently, the MTS reagent was added 20 μl/well, and the plates were incubated for an additional 1–4 h before measuring absorbance at 490 nm.

Generation of Mutated CD20 Molecules. Human CD20 and CD37 cDNA were amplified from Daudi cells and human peripheral blood, respectively, and cloned into plasmid pCI_{NEO} (Promega). Overlap extension PCR was used to generate the CD20 internal deletion mutants $CD20WN_{216-226}$ and $CD20SE_{230-245}$ and CD20.37 chimera. Fluorescent-tagged CD20/CD37 constructs were cloned into pEYFP-C1 (Clontech, Palo Alto, CA).

CD20 and CD37 constructs were transiently transfected into 293T cells using Geneporter (Gene Therapy System, San Diego, CA). In brief, 3×10^5 293T cells in 35-mm wells (Nunc, Denmark) were transfected with 10 μg of DNA using 20 μl of Geneporter reagent. After 24–48 h, cells were washed with PBS and removed for use in various assays. Expression of the constructs was determined by flow cytometry.

Transfection of EHRB, Raji, BL60, and Daudi Cells. Transfection of EHRB, BL60, Raji, or Daudi cells with pEF plasmids encoding Flag-tagged crmA (27) or Bcl_2 (28) vectors, kindly donated by Drs. Andreas Strasser and David Huang, was achieved via electroporation using standard electroporation techniques. Selection with geneticin (1–2 mg/ml) or puromycin (1 μg/ml) was applied 24–48 h later. Expression of the relevant molecule was determined by RT-PCR, Western blot, or intracellular flow cytometry. Flag-tagged crmA was detected by RT-PCR or Western blotting using an anti-Flag Ab (Sigma) as per the manufacturer's instructions. Bcl_2 expression levels were determined by flow cytometric intracellular staining methods using an anti-Bcl_2 Ab (BD PharMingen, San Diego, CA) according to the manufacturer's instructions.

Generation of Cell Cytoplasts. Cell cytoplasts were generated essentially as detailed by Roos *et al.* (29). Briefly, cells were centrifuged through a discontinuous Ficoll-70 (Sigma) gradient (12.5, 16, and 25%) prewarmed to 37°C, containing 5–10 μg/ml cytochalasin B (Sigma) at $81,000 \times g$. After centrifugation, the top band of cellular material was collected. This band was composed of cytoplasts, as assessed by light microscopy, lack of mitochondrial staining with Dioc6 (see above), and absence of DNA as detailed with the DNA fragmentation method detailed above. Cytoplasts were incubated at 1×10^6/ml in the presence or absence of mAb (10 μg/ml) for 16 h at 37°C before being assessed by the annexin V assay.

Table 1 *Specificity, isotype, and source of mAb used in this study*

mAb	Specificity	Isotype	Source
2H7	CD20	IgG2b	Serotec, Oxford, UK
IF5	CD20	IgG2a	ECACC Hybridoma
B1	CD20	IgG2a	Coulter, Miami, FL
HI47	CD20	IgG3	ECACC Hybridoma
Rituximab	CD20	Chimeric Hu Fcγ1	IDEC, San Francisco, CA
AT80	CD20	IgG1	In-house
LT20	CD20	IgG1	Alexander Filatov (24)
11B8	CD20	Hu Fcγ1	Genmab, Utrecht, Holland
ZL7/5	BCR	IgG1	In-house
MB1/7	CD37	IgG1	Richard Miller (49)
WR17	CD37	IgG2a	Keith Moore (50)
1B4	CD38	IgG2a	Fabio Malavasi (51)
L0B3/11	CD95	IgG1	In-house
RFB9	CD19	IgG1	Peter Amlott (52)

RESULTS

Ability of Different Anti-CD20 mAb To Induce Apoptosis in a Range of B-cell Lines. Initially, we assessed the ability of a panel of anti-CD20 mAb to evoke apoptosis in a range of B-cell lines and showed that 24-h post-treatment was optimal to measure apoptosis (data not shown). The apoptotic effect of anti-CD20 mAb on Daudi, EHRB (Ramos), and Raji cells was then assessed by flow cytometry using annexin V (Fig. 1, *A* and *B*). When the mAb was added in free solution without additional cross-linking, a hierarchy of efficacy was observed; 1F5 induced very little apoptosis, while Ritux, like most anti-CD20 mAb (LT20, 2H7, and HI47; data not shown), induced a small degree of apoptosis, and B1, AT80, and to a lesser extent 11B8 induced the highest level of apoptosis. Similar results were observed by flow cytometry when apoptosis was assessed using FSC and PI parameters (data not shown).

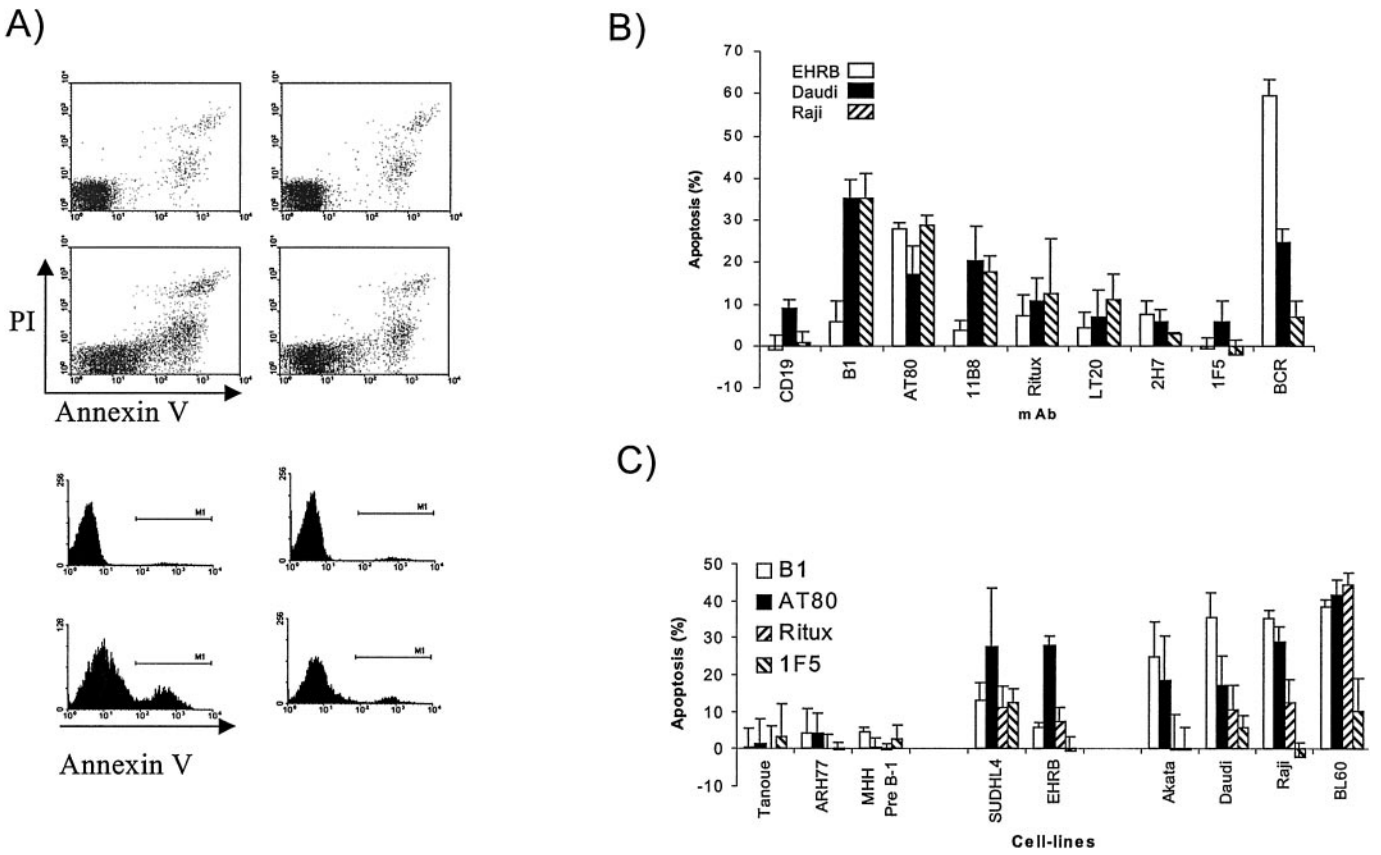

Fig. 1. Apoptosis induced in a range of cell lines by anti-CD20 mAb. Apoptosis was assessed using the annexin V/PI assay 24 h after incubation with anti-CD20 mAb (10 μg/ml). *A*, an example of the dot plots generated (shown for EHRB cells); *B*, a barchart summary of the data from EHRB, Daudi, and Raji cell lines. *C*, apoptosis assessed after incubation of cell lines with B1, AT80, Ritux, and 1F5 (10 μg/ml). Shown are the means and SD of at least three independent experiments.

In EHRB cells, the extent of B1 apoptosis was unexpectedly low, indicating a mAb- and cell-based specificity for apoptosis sensitivity. Therefore, we assessed a wider range of B-cell lines with four of the mAb: (*a*) 1F5; (*b*) Ritux; (*c*) AT80; and (*d*) B1. Three distinct patterns of efficacy were observed (Fig. 1*C* and summarized in Table 2). In type 1 cells (Namalwa, ARH77, Tanoue, and MHH Pre B-1), very little apoptosis was observed after the addition of any of the anti-CD20 mAb. In type 2 cells, moderate levels of apoptosis were observed (EHRB and SUDHL4) with AT80 being the most potent mAb, whereas in type 3 cells, high levels of apoptosis were seen with B1 and AT80 (Akata, BL60, Daudi, and Raji cell lines). Interestingly, both Ritux and B1 induced similar levels of apoptosis in both the SUDHL4 and EHRB cell lines (data not shown and Fig. 1, *B* and *C*). EHRB are a Ramos subline, and Ramos and SUDHL4 cells have been commonly used to study CD20-induced apoptosis, perhaps explaining the view that all anti-CD20 mAb induce similar levels of apoptosis (13). However, in almost all other cells, B1 appeared to be the most effective anti-CD20 mAb, followed by AT80, both of which were more effective than Ritux. In our experiments, no correlation was seen between the sensitivity of cells to anti-BCR and anti-CD20 mAb-induced apoptosis (Table 2), in contrast to that shown by Mathas *et al.* (19). To address whether the different apoptotic effects were translated into longer term consequences, 48-h growth inhibition and 8–12-day clonogenic assays were performed with a subset of the mAb. The experiments are shown in Fig. 2, *A* and *B*, respectively, and reveal that the results of these longer term assays mirrored the apoptosis results such that B1 produced the most profound effects in reducing Daudi cell growth and clonogenicity. AT80 performed similarly to B1 in the growth inhibition assay but was less potent in clonogenicity, whereas 1F5 and Ritux gave much more modest inhibition in both assays.

Table 2 *Sensitivity of various B lymphoma cell lines to anti-CD20 mAb*

Cells were plated out at 2.5–5 $\times$ 10^6/ml in the presence of various anti-CD20 mAb (shown in Fig. 1), and the extent of apoptosis was assessed 24 h later using the annexin V/PI assay. Cells were judged to be insensitive (−), weakly sensitive (+), moderately sensitive (++), or very sensitive (+++).

			Expression level		Sensitivity to Apoptosis	
Cell line	Cell type	EBV status	CD20	sIg	CD20	BCR
Namalwa	BL	+	+	++	−	+
MHH PRE B-1	B-NHL	+	++++	++	−	−
ARH77	MM	+	+++	+	+/−	−
Tanoue	ALL	−	++	+	+/−	+/−
SUDHL4	B-NHL	−	++++++	−	++	+/−
EHRB	BL	+	+++	+	++	++++
Ramos	BL	−	++++	++	++	++
WW2	LCL	+	+++	++	++	ND
Akata	BL	+	+++	+	+++	−
BL60	BL	+	+++	++	+++	++
Raji	BL	+	+++	+	+++	+
Daudi	BL	+	++++	+++	+++	++

BL, Burkitt's lymphoma; LCL, EBV-transformed lymphoblastic B cell line; NHL, Non Hodgkin's Lymphoma, ALL, acute lymphoblastic leukemia; MM, multiple myeloma.

CD20-induced Apoptosis Correlates with Homotypic Cell Adhesion. These differences in mAb performance prompted us to investigate whether similar differences in levels of cell adhesion might be observed. Microscopic analysis of cells after anti-CD20 mAb binding revealed that those mAb which were most potent at inducing apoptosis also induced greater homotypic cellular adhesion (Table 3). Furthermore, in cells where CD20 stimulation did not induce apo-

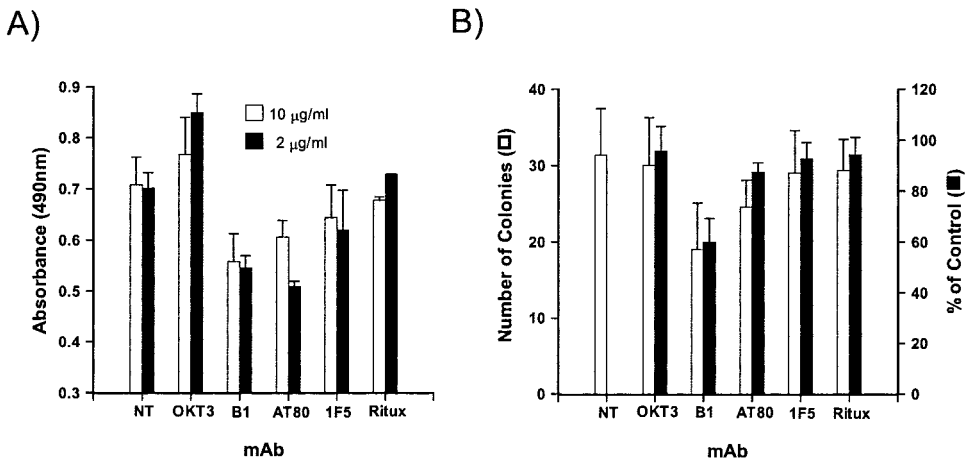

Fig. 2. *A*, growth inhibition of Daudi cells measured by MTS assay. After treatment (48 h) with 10 (□) or 2 (■) μg/ml mAb, cells were incubated with MTS reagent for 1 h, and then the wells were measured for absorbance at 490 nm. Bars represent average values from duplicate wells with the error bars representing the SEM, taken from one of three similar experiments. *B*, clonogenicity of Daudi cells 8–12 days after treatment with anti-CD20 mAb. Two cells per well were seeded in the presence or absence of 5 μg/ml mAb for 8–12 days, and then the number of wells containing colonies scored (□) and calculated as a percentage of the number seen in the control, NT group (■). Shown are the means and SD of three independent experiments.

ptosis (Tanoue), little aggregation was observed, strengthening the link between apoptosis and cellular adhesion.

This aggregation could be partially blocked with anti-LFA-1 mAb, as in previous reports (30). Importantly, this diminished adhesion did not cause decreased apoptosis, indicating that it is the epitope of the mAb and/or its mode of binding that is important for apoptosis rather than homotypic adhesion *per se*. In support of this suggestion, a pan anti-MHCII mAb (F3.3) also caused extensive aggregation in these assays but did not yield correspondingly high levels of apoptosis (data not shown).

CD20-induced Apoptosis Correlates with the Level of mAb Binding. It has been suggested previously that the two hallmark anti-CD20 mAb, 1F5 and B1, bind to distinct epitopes (31) and that this results in different effects. Given the diversity of the apoptotic and aggregative effects induced by our anti-CD20 mAb, we speculated that this also might be caused by differences in epitope binding. To address this question, we carried out cross-blocking studies. These experiments revealed that preincubation with any anti-CD20 mAb blocked the binding of subsequently added FITC-labeled anti-CD20 mAb (data not shown) in agreement with other reports (32, 33), demonstrating that the gross epitope bound by all anti-CD20 mAb is similar or proximal. However, these experiments did reveal an interesting binding phenomenon, essentially that mAb could be grouped according to the extent of their surface binding. FITC-labeled mAb bound either at maximal (LT20, Ritux) levels (average MFI of 770 +/− 30 and 675 +/− 40, respectively) or half-maximal (AT80, B1) levels (average MFI of 250 +/− 25 and 300 +/− 30, respectively) on Daudi cells. Intriguingly, this grouping also appeared to distinguish those mAb that were effective at inducing apoptosis (B1, AT80) from those with lower potency (Ritux, LT20). Subsequently, we extended these observations to a range of cells to determine whether this effect was mAb or cell line specific. These experiments were performed using an indirect flow cytometric method with anti-CD20 mAb followed by a common FITC-labeled secondary agent to remove any experimental variation associated with direct fluoresceination of the different anti-CD20 mAb. These data, shown for B1 and LT20 mAb, representing each type, in Fig. 3*A* demonstrate that the same binding pattern (half-maximal or maximal) was observed in all cell lines tested, indicating a mAb- rather than cell line-specific phenomenon.

To better study this observation and eliminate any misinterpretation caused by the wash steps during the procedure, saturation binding experiments with radiolabeled mAb were performed. As partly reported previously (24) and shown in Fig. 3*B*, B1 and Ritux, despite binding to the same target, CD20 extracellular loop with high affinity, saturate at distinct levels, with Ritux binding almost twice as many molecules on each cell. 1F5 has a lower binding affinity but reaches similar maximum levels of binding to those achieved by Ritux, whereas AT80, although of lower affinity, saturated at the half-maximal level of CD20 binding like B1 (Fig. 3*B*). Several other anti-CD20 mAb were also tested in this binding assay, such as LT20 and 2H7, with similar results to those seen for Ritux and 1F5, whereas 11B8 generated a B1-like binding profile (data not shown). Subsequently, we assessed binding of $F(ab')_2$ and Fab′ fragments of some of these mAb in similar binding assays, expressed as Scatchard plots in Fig. 3*C*. Importantly, although both B1 and Ritux $F(ab')_2$ bound different numbers of molecules from each other, each Fab′ bound twice as many molecules on the cells as the corresponding $F(ab')_2$, indicating that both mAb bind bivalently. Therefore, this half-maximal binding configuration of certain anti-CD20 mAb appears to facilitate the induction of greater levels of apoptosis in sensitive cells. We are currently investigating the molecular differences and consequences of the two different modes of binding.

Movement of CD20 into TX-100 Insoluble Membrane Rafts Does Not Correlate with Apoptosis. We have recently shown that the ability of anti-CD20 mAb to redistribute CD20 into membrane rafts correlates closely with their ability to activate complement and mediate CDC (24). Presumably, this function relates to the binding properties of the mAb, which itself appears to correlate with the degree of apoptosis induced. Therefore, we attempted to correlate the ability of anti-CD20 mAb to translocate CD20 into rafts, using a rapid flow cytometric assay characterized previously (24), with their ability to induce apoptosis. The data (Fig. 4, *A* and *B* for EHRB cells) reveal that some mAb, which are extremely poor at inducing apoptosis (LT20), were potent at redistributing CD20 into membrane rafts, whereas others, such as B1 and 11B8, which were potent in apoptosis assays, were ineffective at causing CD20 redistribution. AT80 was active in both assays, and so movement of CD20 into TX-100 insol-

Table 3 *Homotypic cellular adhesion induced by anti-CD20 mAb*

For adhesion assays, cells were resuspended at 2.5×10^5 cells/ml in the presence of different anti-CD20 mAb at 10 μg/ml and assessed for aggregation after 6–8 h. Increasing aggregation was assessed by the extent and size of cellular aggregates and is designated with an increasing number of +.

		Cell line			
mAb	Isotype	EHRB	Daudi	Raji	Tanoue
NT	−	−	−	+	−
LT20	IgG1	+	+/−	++/+	−
AT80	IgG1	+++/++	++	++	+
B1	IgG2a	++	+++	+++	+
Ritux	Hu IgG1	+	+	++	+/−
11B8	Hu IgG1	++/+	+++	++/+	−

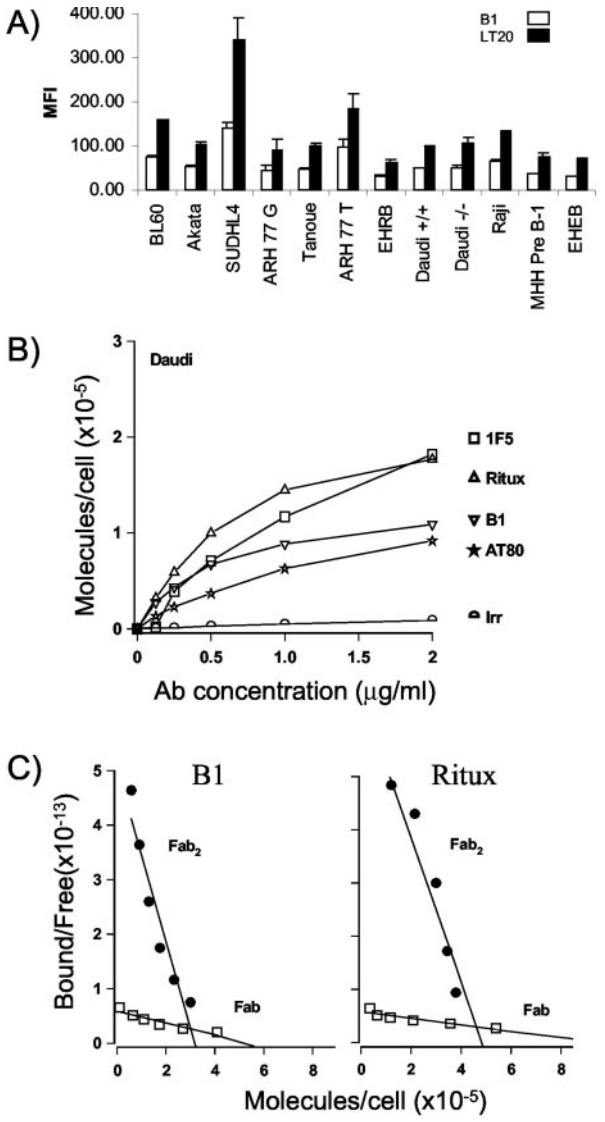

Fig. 3. Binding of anti-CD20 mAb and mAb fragments to B-cell lines measured by flow cytometry and ^{125}I-labeled mAb binding. *A*, anti-CD20 mAb (10 μg/ml) was added to a range of different cell lines for 15 min at 37°C, washed, and then incubated with FITC-labeled goat antimouse IgG F(ab′)$_2$ fragments for 15 min on ice. After washing, cells were assessed by flow cytometry with the MFI shown. Shown are means and SD of three separate experiments. *B* and *C*, ^{125}I-labeled F(ab)′ or F(ab′)$_2$ fragments of anti-CD20 or control (anti-CD3) mAb were incubated with EHRB cells for 2 h at 37°C. The cell-bound and free ^{125}I-labeled mAb were then separated by centrifugation through phthalate oils, and the cell pellets together with bound Ab counted for radioactivity. Data are represented as saturation plots in *B* and Scatchard plots in *C*.

uble rafts appears independent of apoptosis. Similar results were obtained using discontinuous sucrose density gradients followed by SDS-PAGE to isolate rafts and Western blotting for CD20 (data not shown and Ref. 24). NB: The low binding level of 1F5 seen in Fig. 4*A* is attributed to its low affinity and removal by wash steps throughout the assay.

Next, we assessed whether the movement of CD20 into rafts after mAb binding to cells might vary depending on their sensitivity to apoptosis. Therefore, we determined raft redistribution in cells that were unresponsive (MHH PRE B-1, Tanoue, ARH77), moderately responsive (SUDHL4, EHRB), or highly responsive (Raji, BL60, Daudi) to CD20-induced apoptosis. These data, shown in Fig. 4*C* for LT20 and B1 as archetypal good or poor CD20 redistributors, respectively, reveal that CD20 was redistributed in the same pattern and, to a similar extent, in different cell lines, irrespective of their sensitivity to CD20-induced apoptosis. This implies that redistribution of CD20 into TX-100 insoluble membrane rafts does not correlate with sensitivity to CD20-induced apoptosis.

To address the question of raft importance more formally, we constructed a range of mutant or truncated CD20 molecules (detailed in Fig. 5*A*). Polyak *et al.* (34), have previously shown that a region of the CD20 COOH-terminal intracellular tail from residues 219 to 252 is important for raft redistribution. Therefore, we generated two mutant CD20 molecules lacking portions of this region, from residues 216 to 226 and 230 to 245, designated $WN_{216-226}$ (CD20WN) and $SE_{230-245}$ (CD20SE), respectively. As an additional control, we generated a chimeric molecule of CD20 and CD37, swapping the COOH-terminal tail of CD37 for that of CD20 (CD37-CD20 tail). CD37 was chosen as the chimeric partner because it is another tetraspan molecule, with internal COOH and NH_2 termini, that is expressed in B cells but does not induce apoptosis after cross-linking with mAb. These mutant, chimeric,

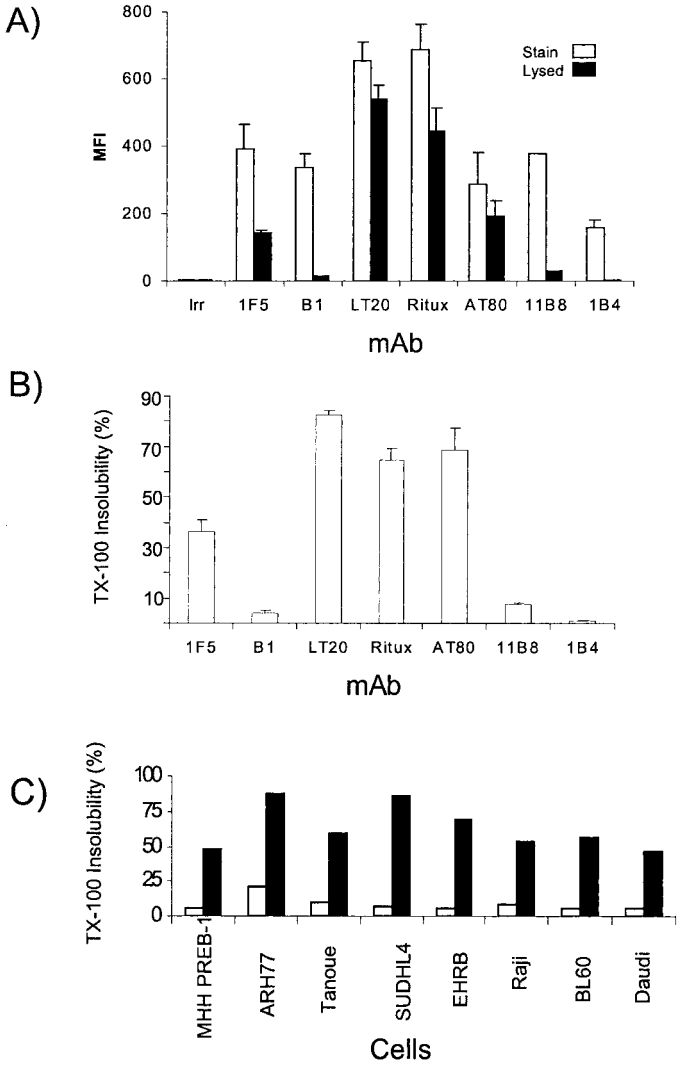

Fig. 4. TX-100 insolubility of CD20 after binding of anti-CD20 mAb. EHRB cells were incubated with 10 μg/ml FITC-mAb for 15 min at 37°C, before washing and dividing the sample in half. One half was maintained on ice in PBS (*x*; *open bars*) allowing calculation of 100% binding levels, whereas the other was treated with 0.5% TX-100 for 15 min on ice (*y*; *filled bars*). Cells were then washed once, resuspended, and assessed by flow cytometry. Shown are MFI values (*A*) and the % TX-100 insoluble fraction (*B*) calculated from using the formula % TX-100 insoluble = (y/x) × 100 (*A*). *C*, shown are means and SD of three independent experiments. Various cell lines were treated with FITC-labeled B1 or LT20 (10 μg/ml) for 15 min at 37°C, and then the samples were treated as for *B*.

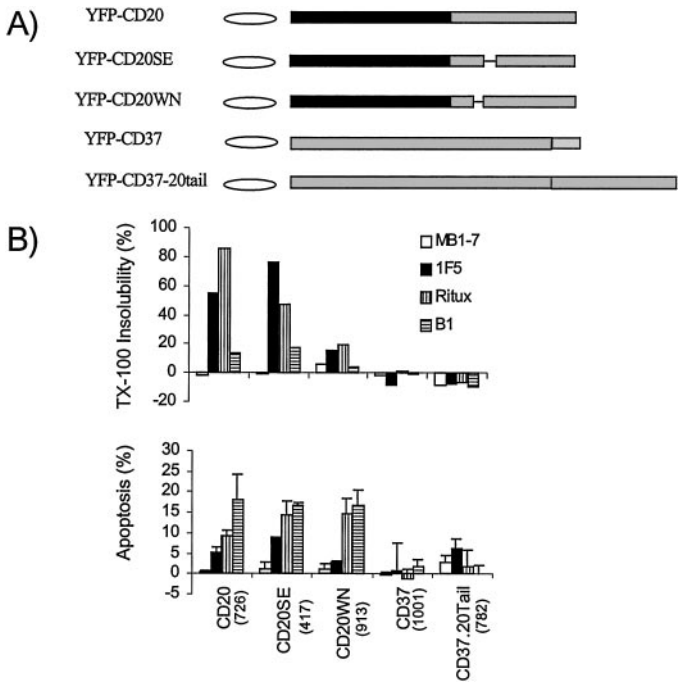

Fig. 5. Effect of the cytoplasmic tail of CD20 on redistribution to membrane rafts and subsequent apoptosis. 293T cells were transfected with various constructs, shown in *A*, and then 24 h later, construct expression was analyzed by flow cytometry in FL1 (MFI values given in parentheses in *B*). For raft redistribution assay (*top panel*), the transfected cells were incubated with 10 μg/ml Ab at 37°C for 30 min, washed, and added to ice cold 0.5% TX-100 lysis buffer. The mixture was further incubated at 4°C for 30 min. After washing twice with ice cold PBS, the MFI of the lysed transfectants was assessed by flow cytometry and expressed as a percentage of a nonlysed sample. For the mAb-induced apoptosis assay (*bottom panel*), the cells were added to a 24-well plate (coated with 10 μg/ml Ab in PBS at 37°C for 5 h) at 2×10^5/well. After an additional 24-h incubation, the cells were harvested, and the percentage of apoptotic cells was determined by FSC and PI criteria via flow cytometry. Shown are the means and SD of triplicate samples from a single experiment. These experiments were repeated at least three times with similar results.

and wild-type CD20 molecules were tagged with the fluorescent reporter protein YFP to facilitate their detection. After expressing these molecules in 293T cells, various anti-CD20 mAb were added, and the extent of raft redistribution was assessed. These experiments, shown in the top panel of Fig. 5*B* for a subset of the mAb used, revealed that the pattern of redistribution for the different anti-CD20 mAb was similar in transfected 293T cells to that for endogenous CD20 in the B-cell lines (Fig. 4), such that Ritux and 1F5 induced redistribution but B1 did not. As expected, although all of the CD20 molecules were similarly expressed (MFI are shown in parentheses under the graph for each construct), the extent of raft redistribution was greatly diminished in the CD37 chimera (which is bound by an anti-CD37 mAb but not by anti-CD20 mAb), the CD20WN mutant, and, to a lesser extent, the CD20SE mutant. Neither wild-type CD37, nor the CD37-CD20 tail construct, were redistributed by binding of an anti-CD37 mAb (MB1/7). Given this information, the chimeric and mutant molecules were then compared in a cell death assay after ligation with these different mAb. Cell death was determined with the viability dye PI, as annexin V FITC, could not be used in the presence of YFP. These data shown in the bottom panel of Fig. 5*B* reveal that similar levels of cell death were observed in the three CD20 constructs (CD20, CD20WN, and CD20SE), indicating that redistribution of CD20 into the TX-100 insoluble membrane fraction is not necessary for subsequent apoptosis. As expected, the CD37 molecules did not induce substantial apoptosis when ligated.

CD20-induced Apoptosis Appears Independent of Caspase Activity. Next, we determined which pathway of apoptosis anti-CD20 mAb may induce. In experiments, anti-CD20 mAb did not induce high levels of DNA fragmentation either when added in free solution or when immobilized to enhance cross-linking (Fig. 6*A* and data not shown). This is unlikely to reflect the inability of our cell lines to undergo DNA fragmentation *per se,* because anti-BCR mAb were able to induce fragmentation in EHRB cells 48 h after treatment, and cycloheximide induced fragmentation in all three lines assessed (Fig. 6*A*). Given this low level of DNA fragmentation, we wanted to address whether caspases were activated after CD20 ligation. Caspase-3 is one of the terminal caspases involved in cellular destruction, so we assessed its processing in EHRB cells after treatment with anti-CD20, -BCR, or CD95 mAb. EHRB cells were chosen because they are sensitive to all of these stimuli (data not shown). These data show that caspase-3 was cleaved after each of the three stimuli (Fig. 6*B*). Caspase-3 is a downstream caspase involved in final cellular destruction, and we wondered whether other caspases might play a role in the initiation of the apoptotic cascade, similar to that seen with CD95. Therefore, we transfected EHRB cells with the serpin molecule crmA, a potent inhibitor of initiator caspases-8 and -10, and assessed these cells for sensitivity to apoptosis. As shown in Fig. 6*C,* crmA was expressed in transfected cells and potently inhibited CD95 apoptosis but was ineffective in inhibiting BCR- or CD20-mediated cell death. Similar results were obtained with Raji cell transfectants (data not shown; anti-BCR is ineffective in these cells). Next, we used the cell-permeable caspase inhibitor tetrapeptide ZVAD-FMK to determine whether caspases other than caspase-8 and -10 were involved. These experiments revealed that ZVAD over a range of concentrations from 0.4 to 50 μM was a potent inhibitor of CD95-induced apoptosis, partially effective at reducing BCR apoptosis, but completely unable to prevent CD20-induced apoptosis (Fig. 6*D*), and even concentrations of 200 μM were unable to prevent PS translocation after CD20 stimulus (data not shown). As ZVAD-FMK is a poor inhibitor of caspase-2, we also assessed the efficacy of a specific caspase-2 inhibitor (VDVAD), which was similarly ineffective (Fig. 6*D*). The same inhibitors were assessed on a range of other cells (Daudi, Raji, and BL60), and similar results were observed (data not shown). Taken together, these data infer that caspases are not involved in the initiation events of apoptosis triggered through CD20.

CD20-induced Apoptosis Is Only Partially Regulated by Mitochondria and Blocked by Bcl_2. Given the apparent lack of caspase involvement in signaling for CD20-induced apoptosis, we wished to assess the role of mitochondria in the death process. In preliminary experiments with the mitochondrial reporter dyes JC-1 or DioC6, we revealed that cells triggered to undergo apoptosis with CD20 did appear to undergo the MPT as judged by a decrease in green fluorescence (Fig. 7*A*). To address the importance of mitochondria in CD20-induced apoptosis more formally, we also chose to compare the effects of anti-CD20 mAb in wild-type cells and cells transfected with the archetypal antiapoptotic mitochondrial protein Bcl_2 (expression levels shown as an *inset* in Fig. 7*B*). These experiments were again performed in conjunction with CD95- and BCR-apoptotic stimuli as controls. As shown (Fig. 7*C*), all three ligands induced the MPT and in a similar proportion of cells to that seen with annexin V. Bcl_2 inhibited the number of cells undergoing the permeability transition but had only a minor effect on reducing the number of annexin V-positive cells after CD20 stimulation. CD95 and, to a lesser extent, BCR-induced annexin V positivity was reduced by Bcl_2. These data indicate that, although Bcl_2 controls the mitochondrial changes in transfectant cells, it is not

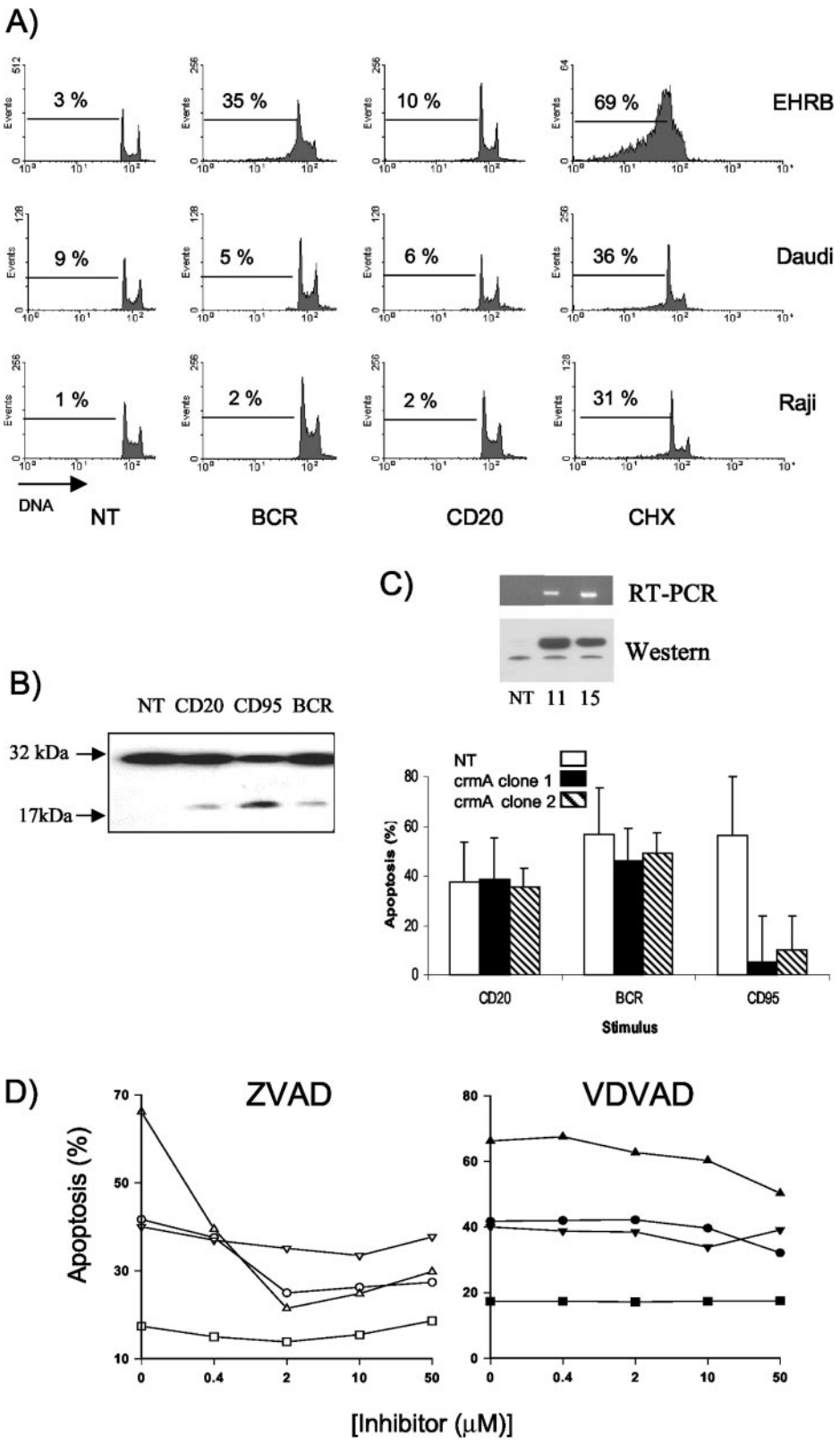

Fig. 6. Involvement of caspases in apoptosis induced by CD20, BCR, and CD95 ligation. *A*, DNA fragmentation determined by hypotonic PI assay in EHRB, Daudi, or Raji cells after 48-h stimulation with 10 μg/ml anti-CD20 (AT80), anti-BCR (ZL7/5), or Cycloheximide (*CHX*). *B*, processing of caspase-3 determined by Western blotting for caspase-3, in EHRB cells 24 h after stimulation with 10 μg/ml anti-CD20 (AT80), anti-BCR (ZL7/5), or anti-CD95 (LOB3/11) or no treatment (*NT*). Cells were harvested, lysed, and electrophoresed before transfer and Western blotting. Shown are the processed (17 kDa) and unprocessed (32 kDa) bands of caspase-3. *C*, effect of crmA on apoptosis induced by 10 μg/ml anti-CD20 (AT80), anti-BCR (ZL7/5), or anti-CD95 (LOB3/11). Nontransfected (*NT*) or two separate clones of EHRB cells, expressing crmA, shown in the *inset* by RT-PCR and Western blotting, were assessed for apoptosis as assessed by annexin V staining. Shown are the means and SD of at least three independent experiments. *D*, effect of ZVAD (*open symbols*) and VDVAD (*closed symbols*) on the apoptosis induced in 24 h by inhibitor alone (□), 10 μg/ml anti-CD20 (▽, AT80), anti-BCR (○, ZL7/5), or anti-CD95 (△, LOB3/11) in EHRB cells. Inhibitors (*ZVAD* and *VDVAD*) were added over a range of different concentrations for 2 h before the addition of mAb. Shown are means and SD of at least three experiments.

sufficient to inhibit PS translocation after CD20 ligation. BL60 and Daudi cells were also transfected with Bcl_2, and similar results were observed (data not shown).

As an alternative approach to show that CD20-induced apoptosis bypasses mitochondria, we generated cell cytoplasts, which lack mitochondria. Cells or cytoplasts from Daudi cells were incubated with different mAb, and annexin V binding was assessed 18 h later. Anti-CD20 mAb triggered an increase in annexin V staining in cytoplasts, to a similar extent to that seen in whole cells (Fig. 7*D*). Importantly, mAb that were inert on cells (anti-CD95) were also inert on cytoplasts (data not shown). Altogether, these data indicate that ligation of CD20 can induce apoptosis (as judged by an

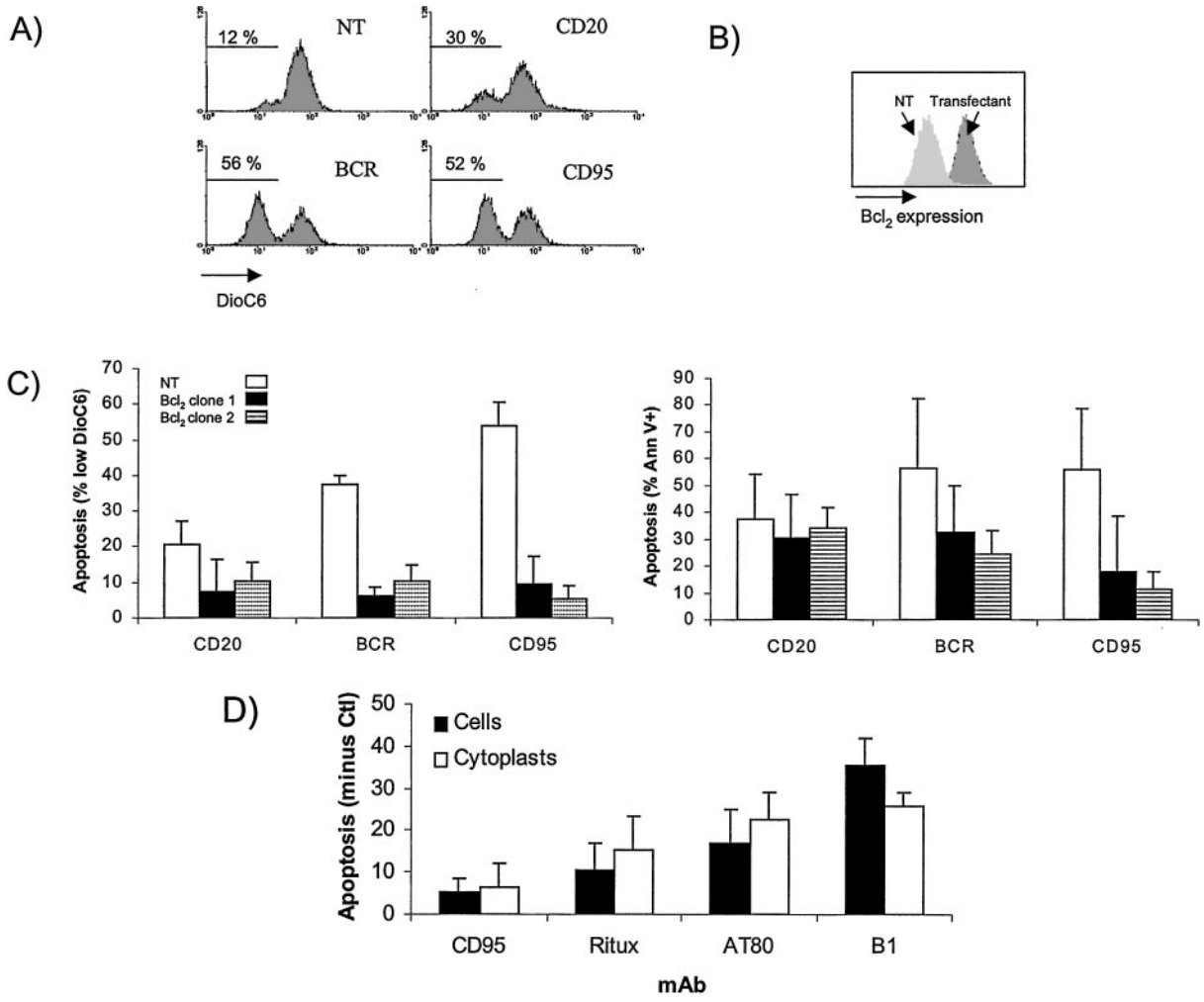

Fig. 7. Involvement of mitochondria in apoptosis induced by CD20, BCR, and CD95 ligation. *A*, 10 μg/ml anti-CD20 (AT80), anti-BCR (ZL7/5), or anti-CD95 (LOB3/11) were added to EHRB cells for 24 h, and then the extent of mitochondrial permeability change was assessed with the reporter dye DioC6. Cells displaying low levels of fluorescence are judged to have undergone the transition, and the percentage of such cells is shown in each case. *B*, expression of Bcl_2 in transfectant clones assessed by intracellular staining compared with nontransfected (*NT*) cells. *C*, effect of Bcl_2 on apoptosis induced by 10 μg/ml anti-CD20 (AT80), anti-BCR (ZL7/5), or anti-CD95 (LOB3/11). Nontransfected (*NT*) or two separate clones of EHRB cells, overexpressing Bcl_2, as shown in *B*, were assessed for apoptosis as assessed by annexin V or DioC6 staining. Shown are the means and SD of at least three independent experiments. In *D*, cytoplasts were generated from Daudi cells by cytochalasin B treatment, washed, and then incubated with 10 μg/ml anti-CD20 (B1, AT80. Ritux) or anti-CD95 mAb (LOB3/11) for 16–18 h before staining with annexin V. As a comparison, whole cells were also treated. Shown are the means and SD of four experiments.

increase in annexin V staining) in sensitive cell lines in the absence of mitochondria.

DISCUSSION

The ability of anticancer mAb to evoke target cell apoptosis appears to be a desirable trait and may distinguish those mAb which are successful in the clinic from those which are not (35). Intracellular signaling is also thought to be important for subsequent therapeutic responses (36). Based on the finding that Ritux can redistribute CD20 to the TX-100 insoluble lipid membrane compartment of the cell, where many important signaling enzymes and mediators are located, it would be expected that CD20 transduces its apoptotic signal in this compartment. However, we show that this is not the case and that in fact redistribution of CD20 to the TX-100 insoluble compartment appears independent of any subsequent apoptotic response.

B1, along with our own mAb AT80 and 11B8, is potent at inducing apoptosis in a number of different B-cell lines, whereas most anti-CD20 mAb are only weakly or nonapoptotic, without hyper-cross-linking. Although these mAb are different in affinity, isotype, and the ability to redistribute CD20 into TX-100 insoluble membrane rafts, one common property is their mode of binding. B1, 11B8, and AT80 all bind at a half-maximal level compared with all other anti-CD20 mAb thus far tested. Presumably then, their apoptotic efficacy is related to how or in what conformation they bind CD20. CD20 is thought to form multimers on the cell surface, with dimers, tetramers, and larger complexes detected after chemical cross-linking and detergent lysis experiments (37, 38). Despite our lack of understanding of how such binding occurs, this difference in binding affords these mAb an increased capacity to evoke apoptosis in sensitive cells.

However, this property does not seem to be fully related to the ability of the mAb to induce potent cross-linking of CD20. Although both B1 and 11B8 do not redistribute CD20 into TX-100 insoluble regions of the membrane, a property which we showed previously to be related to the extent of cross-linking (24), AT80 does, and so the binding pattern of these mAb appears independent of cross-linking. Half-maximal binding and apoptosis also appear to correlate with the degree of homotypic adhesion. This in turn may indicate that an enhanced level of signaling is evoked when anti-CD20 mAb bind in this conformation. The nature of the signals transduced after different

(apoptotic and nonapoptotic) mAb and how apoptosis is affected forms the basis of our ongoing studies.

It is intriguing to note that although caspase-3 is cleaved during CD20-induced apoptosis, caspases are apparently not important for the cell death. Neither crmA nor caspase inhibitors were able to significantly inhibit anti-CD20-induced apoptosis as measured by annexin V or DioC6 staining, although they were active against other inducers of apoptosis, such as anti-CD95. Others have reported that CD20-induced apoptosis is dependent on caspase activation, but in almost all of these studies, late stage apoptosis (DNA fragmentation) was assessed after hyper-cross-linking in the presence of noncaspase-specific concentrations of ZVAD (>50 μM; Refs. 18 and 19). In our experiments, additional cross-linking did not always induce substantial improvements in apoptosis, and the effect was variable both for mAb and cells (data not shown). Interestingly, a recent study showed that BCR apoptosis signaled through soluble mAb binding was caspase independent, whereas hyper-cross-linking induced the involvement of caspases (39). Potentially then, caspase involvement in CD20-induced apoptosis is caused by the artificial levels of hyper-cross-linking used.

The lack of caspase involvement may explain why only low levels of DNA fragmentation are observed after anti-CD20 mAb ligation. Similar results were reported by Rose *et al.* (40) recently for Ritux in a range of cell lines where no further cross-linking was provided. However, the low level may also be partly explained by the fact that DNA fragmentation is a relatively late event in the cell death process. Furthermore, anti-CD20 treatment induces only a subpopulation of cells to undergo apoptosis, whereas the remainder continues to proliferate, seemingly unaffected, and repopulate the culture. In comparison, both anti-BCR and anti-CD95 mAb cause apoptosis, which increases over time, finally affecting almost all cells in the culture. Therefore, the proportion of cells undergoing DNA fragmentation after anti-CD20 treatment may be masked by the unaffected/newly divided cells.

Another unusual property of CD20-induced apoptosis involves the mitochondria. Although CD20-triggered apoptosis clearly progresses through the mitochondria as judged by the induction of the MPT, overexpression of Bcl_2 was only partially able to block the apoptotic effects of anti-CD20 mAb. This phenomenon was also very recently reported by Van der Kolk *et al.* (41) in Ramos cells and observed by us in three separate cell lines and so does not represent an artifact of Ramos cells. Therefore, CD20 may engage a novel caspase-independent apoptotic pathway that is also partly independent of the usually strict mitochondrial controls.

Although direct evidence supporting the involvement of CD20 as a Ca^{2+}channel is not extensive (37), and Ca^{2+} flux is only apparent after additional cross-linking of mAb (42, 43), a broad spectrum signaling molecule, such as Ca^{2+}, could at least be envisaged to have multiple sites of action, allowing a component to be independent of mitochondrial regulation. In agreement with this notion, several authors have shown that apoptosis induced by hyper-cross-linked anti-CD20 mAb can be inhibited by intracellular (BAPTA) and extracellular (EGTA) Ca^{2+} chelators (18, 43).

It was suggested previously that CD20 and BCR stimulation involved similar signaling and apoptotic pathways (19). However, our observations regarding the ability of Bcl_2 to block PS exposure triggered through the BCR but not CD20, and lack of correlation of sensitivity to anti-CD20 and anti-BCR in different cell lines, indicate that CD20 and the BCR use distinct pathways. Furthermore, the difference in signaling evoked through ligation of these two receptors has been known for many years (44).

The proportion of cells assessed as apoptotic in our study was generally higher with annexin V than other measures. Certain authors have speculated on this basis that annexin V binding is a poor measure of apoptosis (11). However, given that annexin V detects the presence of PS asymmetry on the cell surface and that this PS can be recognized by scavenger receptors of macrophages, resulting in cellular engulfment (45, 46), it would seem an important and perhaps physiologically relevant measure of apoptosis, especially when considering the CD20-induced apoptosis *in vivo*.

Here we have shown that TX-100 insoluble membrane rafts are not important for apoptotic transduction. Conversely, we have reported previously that these same TX-100 rafts were extremely important for evoking powerful CDC. As both B1 and 1F5 mAb are similarly potent in ADCC (47), our data here indicate that ADCC, like apoptosis, is also not reliant on redistribution of CD20 to TX-100 insoluble membrane rafts.

It has been suggested recently that rafts other than those detected by TX-100 may exist and that other less harsh detergents, such as BRIJ98, may detect smaller lipid raft domains (48). Presumably on this basis, Deans *et al.* (16) and others[4] (Suzanne Morgan, personal communication) have suggested that CD20 may already reside within membrane rafts before ligation with anti-CD20 mAb. Therefore, it may be that signaling for apoptosis does in fact require membrane rafts but that these rafts are small "mini-rafts" that already surround CD20 in the plasma membrane yet are undetectable by TX-100 extraction methods.

However, what controls sensitivity to CD20 apoptosis remains unclear because binding level (maximal/half-maximal), raft redistribution, EBV status, and CD20 expression level all appear unrelated to it. Presumably, crucial signaling or effector molecules are missing or dysregulated in insensitive cell lines, and it is hoped that a careful study of these will reveal more about the signaling/apoptotic pathway engaged by CD20. One possibility is that the expression level of Cbp/PAG controls the sensitivity of the different cells, because it is known that PAG regulates the kinase activity of CD20 by linking it to Src kinases (15, 42).

Overall, it may be speculated from these and our previous *in vitro* results (4, 47) that one of the central effector mechanisms of Ritux *in vivo* is complement. Interestingly, the other clinically relevant anti-CD20 mAb B1 demonstrates perhaps the most potent apoptotic and least impressive CDC effects of all anti-CD20 mAb tested. Presumably then, B1, used clinically in a radioconjugated form as Bexxar, contributes to therapeutic responses through apoptotic and not complement mechanisms.

ACKNOWLEDGMENTS

We thank all members of the Tenovus Cancer Laboratory who provided expert technical support and valuable discussion. We also thank Drs. Richard Miller, Geoff Hale, Fabio Malavasi, and Alexander Filatov for generously providing mAb and Drs. Andreas Strasser and David Huang for the kind gift of crmA and Bcl_2 vectors. Finally, we thank Dr. Graham Packham, Peter Johnson, and Dr. Jan Van de Winkel for providing technical information and advice during the study.

REFERENCES

1. Gopal, A. K., and Press, O. W. Clinical applications of anti-CD20 antibodies. J. Lab. Clin. Med., *134:* 445–450, 1999.
2. Glennie, M. J., and Johnson, P. W. Clinical trials of antibody therapy. Immunol. Today, *21:* 403–410, 2000.
3. Maloney, D. G., Smith, B., and Rose, A. Rituximab: mechanism of action and resistance. Semin. Oncol., *29:* 2–9, 2002.
4. Leandro, M. J., Edwards, J. C., and Cambridge, G. Clinical outcome in 22 patients with rheumatoid arthritis treated with B lymphocyte depletion. Ann. Rheum. Dis., *61:* 883–888, 2002.

[4] S. Morgan, personal communication.

5. Anderson, D. R., Grillo-Lopez, A., Varns, C., Chambers, K. S., and Hanna, N. Targeted anti-cancer therapy using rituximab, a chimaeric anti-CD20 antibody (IDEC-C2B8) in the treatment of non-Hodgkin's B-cell lymphoma. Biochem. Soc. Trans., *25:* 705–708, 1997.
6. Clynes, R. A., Towers, T. L., Presta, L. G., and Ravetch, J. V. Inhibitory Fc receptors modulate in vivo cytoxicity against tumor targets. Nat. Med., *6:* 443–446, 2000.
7. Cartron, G., Dacheux, L., Salles, G., Solal-Celigny, P., Bardos, P., Colombat, P., and Watier, H. Therapeutic activity of humanized anti-CD20 monoclonal antibody and polymorphism in IgG Fc receptor FcgammaRIIIa gene. Blood, *99:* 754–758, 2002.
8. van der Kolk, L. E., Grillo-Lopez, A. J., Baars, J. W., Hack, C. E., and van Oers, M. H. Complement activation plays a key role in the side-effects of rituximab treatment. Br. J. Haematol., *115:* 807–811, 2001.
9. Bannerji, R., and Flinn, I. W. Cell surface complement inhibitors CD55 and CD59 may mediate chronic lymphocytic leukemia (CLL) resistance to rituximab therapy. Blood, *96:* 164a, 2000.
10. Treon, S. P., Mitsiades, C., Mitsiades, N., Young, G., Doss, D., Schlossman, R., and Anderson, K. C. Tumor cell expression of CD59 is associated with resistance to CD20 serotherapy in patients with B-cell malignancies. J. Immunother., *24:* 263–271, 2001.
11. Manches, O., Lui, G., Chaperot, L., Gressin, R., Molens, J. P., Jacob, M. C., Sotto, J. J., Leroux, D., Bensa, J. C., and Plumas, J. In vitro mechanisms of action of rituximab on primary non-Hodgkin lymphomas. Blood, *101:* 949–954, 2003.
12. Tedder, T. F., Forsgren, A., Boyd, A. W., Nadler, L. M., and Schlossman, S. F. Antibodies reactive with the B1 molecule inhibit cell cycle progression but not activation of human B lymphocytes. Eur. J. Immunol., *16:* 881–887, 1986.
13. Shan, D., Ledbetter, J. A., and Press, O. W. Apoptosis of malignant human B cells by ligation of CD20 with monoclonal antibodies. Blood, *91:* 1644–1652, 1998.
14. Byrd, J. C., Kitada, S., Flinn, I. W., Aron, J. L., Pearson, M., Lucas, D., and Reed, J. C. The mechanism of tumor cell clearance by rituximab in vivo in patients with B-cell chronic lymphocytic leukemia: evidence of caspase activation and apoptosis induction. Blood, *99:* 1038–1043, 2002.
15. Deans, J. P., Robbins, S. M., Polyak, M. J., and Savage, J. A. Rapid redistribution of CD20 to a low density detergent-insoluble membrane compartment. J. Biol. Chem., *273:* 344–348, 1998.
16. Deans, J. P., Li, H., and Polyak, M. J. CD20-mediated apoptosis: signaling through lipid rafts. Immunology, *107:* 176–182, 2002.
17. Sproul, T. W., Malapati, S., Kim, J., and Pierce, S. K. Cutting edge: B cell antigen receptor signaling occurs outside lipid rafts in immature B cells. J. Immunol., *165:* 6020–6023, 2000.
18. Shan, D., Ledbetter, J. A., and Press, O. W. Signaling events involved in anti-CD20-induced apoptosis of malignant human B cells. Cancer Immunol. Immunother., *48:* 673–683, 2000.
19. Mathas, S., Rickers, A., Bommert, K., Dorken, B., and Mapara, M. Y. Anti-CD20- and B-cell receptor-mediated apoptosis: evidence for shared intracellular signaling pathways. Cancer Res., *60:* 7170–7176, 2000.
20. Borner, C., and Monney, L. Apoptosis without caspases: an inefficient molecular guillotine? Cell Death Differ., *6:* 497–507, 1999.
21. Bouchon, A., Krammer, P. H., and Walczak, H. Critical role for mitochondria in B cell receptor-mediated apoptosis. Eur. J. Immunol., *30:* 69–77, 2000.
22. Glennie, M. J., McBride, H. M., Worth, A. T., and Stevenson, G. T. Preparation and performance of bispecific F(ab' gamma)2 antibody containing thioether-linked Fab' gamma fragments. J. Immunol., *139:* 2367–2375, 1987.
23. Tutt, A. L., French, R. R., Illidge, T. M., Honeychurch, J., McBride, H. M., Penfold, C. A., Fearon, D. T., Parkhouse, R. M., Klaus, G. G., and Glennie, M. J. Monoclonal antibody therapy of B cell lymphoma: signaling activity on tumor cells appears more important than recruitment of effectors. J. Immunol., *161:* 3176–3185, 1998.
24. Cragg, M. S., Morgan, S. M., Chan, H. T., Morgan, B. P., Filatov, A. V., Johnson, P. W., French, R. R., and Glennie, M. J. Complement-mediated lysis by anti-CD20 mAb correlates with segregation into lipid rafts. Blood, *101:* 1045–1052, 2003.
25. Vermes, I., Haanen, C., Steffens-Nakken, H., and Reutelingsperger, C. A novel assay for apoptosis. Flow cytometric detection of phosphatidylserine expression on early apoptotic cells using fluorescein labelled Annexin V. J. Immunol. Methods, *184:* 39–51, 1995.
26. Cragg, M. S., Zhang, L., French, R. R., and Glennie, M. J. Analysis of the interaction of monoclonal antibodies with surface IgM on neoplastic B-cells. Br. J. Cancer, *79:* 850–857, 1999.
27. Strasser, A., Harris, A. W., Huang, D. C., Krammer, P. H., and Cory, S. Bcl-2 and Fas/APO-1 regulate distinct pathways to lymphocyte apoptosis. EMBO J., *14:* 6136–6147, 1995.
28. Huang, D. C., Cory, S., and Strasser, A. Bcl-2. Bcl-XL and adenovirus protein E1B19kD are functionally equivalent in their ability to inhibit cell death. Oncogene, *14:* 405–414, 1997.
29. Roos, D., and Voetman, A. A. Preparation and cryopreservation of cytoplasts from human phagocytes. Methods Enzymol., *132:* 250–257, 1986.
30. Kansas, G. S., and Tedder, T. F. Transmembrane signals generated through MHC class II. CD19, CD20, CD39, and CD40 antigens induce LFA-1-dependent and independent adhesion in human B cells through a tyrosine kinase-dependent pathway. J. Immunol., *147:* 4094–4102, 1991.
31. Tedder, T. F., and Engel, P. CD20: a regulator of cell-cycle progression of B lymphocytes. Immunol. Today, *15:* 450–454, 1994.
32. Tedder, T. F., and Penta, A. Structure of the CD20 antigen and gene of human and mouse B-cells: use of transfected cell lines to examine the Workshop panel of antibodies. *In:* W. Knapp, B. Dorken, W. R. Gilks, E. P. Rieber, R. E. Schmidt, H. Stein, and A. E. G. von dem Borne (eds.), Leukocyte Antigens IV, pp. 48–50. Oxford: Oxford University Press, 1989.
33. Clark, E. A., Shu, G., and Ledbetter, J. A. Role of the Bp35 cell surface polypeptide in human B-cell activation. Proc. Natl. Acad. Sci. USA, *82:* 1766–1770, 1985.
34. Polyak, M. J., Tailor, S. H., and Deans, J. P. Identification of a cytoplasmic region of CD20 required for its redistribution to a detergent-insoluble membrane compartment. J. Immunol., *161:* 3242–3248, 1998.
35. Cragg, M. S., French, R. R., and Glennie, M. J. Signaling antibodies in cancer therapy. Curr. Opin. Immunol., *11:* 541–547, 1999.
36. Vuist, W. M., Levy, R., and Maloney, D. G. Lymphoma regression induced by monoclonal anti-idiotypic antibodies correlates with their ability to induce Ig signal transduction and is not prevented by tumor expression of high levels of bcl-2 protein. Blood, *83:* 899–906, 1994.
37. Bubien, J. K., Zhou, L. J., Bell, P. D., Frizzell, R. A., and Tedder, T. F. Transfection of the CD20 cell surface molecule into ectopic cell types generates a Ca2+ conductance found constitutively in B lymphocytes. J. Cell Biol., *121:* 1121–1132, 1993.
38. Polyak, M. J., and Deans, J. P. Alanine-170 and proline-172 are critical determinants for extracellular CD20 epitopes; heterogeneity in the fine specificity of CD20 monoclonal antibodies is defined by additional requirements imposed by both amino acid sequence and quaternary structure. Blood, *99:* 3256–3262, 2002.
39. Besnault, L., Schrantz, N., Auffredou, M. T., Leca, G., Bourgeade, M. F., and Vazquez, A. B cell receptor cross-linking triggers a caspase-8-dependent apoptotic pathway that is independent of the death effector domain of Fas-associated death domain protein. J. Immunol., *167:* 733–740, 2001.
40. Rose, A. L., Smith, B. E., and Maloney, D. G. Glucocorticoids and rituximab in vitro: synergistic direct antiproliferative and apoptotic effects. Blood, *100:* 1765–1773, 2002.
41. van der Kolk, L. E., Evers, L. M., Omene, C., Lens, S. M., Lederman, S., van Lier, R. A., van Oers, M. H., and Eldering, E. CD20-induced B cell death can bypass mitochondria and caspase activation. Leukemia (Baltimore), *16:* 1735–1744, 2002.
42. Deans, J. P., Schieven, G. L., Shu, G. L., Valentine, M. A., Gilliland, L. A., Aruffo, A., Clark, E. A., and Ledbetter, J. A. Association of tyrosine and serine kinases with the B cell surface antigen CD20. Induction via CD20 of tyrosine phosphorylation and activation of phospholipase C-gamma 1 and PLC phospholipase C-gamma 2. J. Immunol., *151:* 4494–4504, 1993.
43. Hofmeister, J. K., Cooney, D., and Coggeshall, K. M. Clustered CD20 induced apoptosis: src-family kinase, the proximal regulator of tyrosine phosphorylation, calcium influx, and caspase 3-dependent apoptosis. Blood Cells Mol. Dis., *26:* 133–143, 2000.
44. White, M. W., Draves, K. E., Morris, D. R., and Clark, E. A. Surface IgM and CD20 receptors utilize distinct signal transduction pathways. *In:* W. Knapp, B. Dorken, W. R. Gilks, D. Mason, A. Pascale, A. Bernsussan, C. Buckley, C. Civin, E. Clark, M. de Haas, S. Goyert, M. Hadam, D. Hart, *et al.* (eds.), Leukocyte Antigens IV, pp. 51–54. Oxford: Oxford University Press, 1989.
45. Fadok, V. A., Voelker, D. R., Campbell, P. A., Cohen, J. J., Bratton, D. L., and Henson, P. M. Exposure of phosphatidylserine on the surface of apoptotic lymphocytes triggers specific recognition and removal by macrophages. J. Immunol., *148:* 2207–2216, 1992.
46. Fadok, V. A., Bratton, D. L., Rose, D. M., Pearson, A., Ezekewitz, R. A., and Henson, P. M. A receptor for phosphatidylserine-specific clearance of apoptotic cells. Nature (Lond.), *405:* 85–90, 2000.
47. Cragg, M. S., O'Brien, L., Tutt, A., Chan, C., Anderson, V. A., and Glennie, M. J. Opposing properties of CD20 mAb. *In:* D. Mason, P. Andre, A. Bensussan, C. Buckley, C. Civin, E. Clark, M. de Haas, S. Goyert, M. Hadam, D. Hart, *et al.* (eds.), Leukocyte Typing VII, pp. 95–97. Oxford: Oxford University Press, 2002.
48. Drevot, P., Langlet, C., Guo, X. J., Bernard, A. M., Colard, O., Chauvin, J. P., Lasserre, R., and He, H. T. TCR signal initiation machinery is pre-assembled and activated in a subset of membrane rafts. EMBO J., *21:* 1899–1908, 2002.
49. Press, O. W., Eary, J. F., Badger, C. C., Martin, P. J., Appelbaum, F. R., Levy, R., Miller, R., Brown, S., Nelp, W. B., Krohn, K. A., *et al.* Treatment of refractory non-Hodgkin's lymphoma with radiolabeled MB-1 (anti-CD37) antibody. J. Clin. Oncol., *7:* 1027–1038, 1989.
50. Moore, K., Cooper, S. A., and Jones, D. B. Use of the monoclonal antibody WR17, identifying the CD37 gp40–45 Kd antigen complex, in the diagnosis of B-lymphoid malignancy. J. Pathol., *152:* 13–21, 1987.
51. Funaro, A., De Monte, L. B., Dianzani, U., Forni, M., and Malavasi, F. Human CD38 is associated to distinct molecules which mediate transmembrane signaling in different lineages. Eur. J. Immunol., *23:* 2407–2411, 1993.
52. Bonardi, M. A., French, R. R., Amlot, P., Gromo, G., Modena, D., and Glennie, M. J. Delivery of saporin to human B-cell lymphoma using bispecific antibody: targeting via CD22 but not CD19, CD37, or immunoglobulin results in efficient killing. Cancer Res., *53:* 3015–3021, 1993.